

## AMELIORATIVE EFFECT OF QUERCETIN NANOPARTICLES ON CYCLOPHOSPHAMIDE-INDUCED HEPATOTOXICITY IN RATS

ARMIA N.M. GHALY<sup>1,2</sup>; MOKHTAR TAHA<sup>2</sup>; ABEER S. HASSAN<sup>3</sup> AND KHALED M.A. HASSANEIN<sup>2</sup>

<sup>1</sup> Department of Pathology and Clinical Pathology, Faculty of Veterinary Medicine, South Valley University, Qena, 83523, Egypt.

<sup>2</sup> Department of Pathology and Clinical Pathology, Faculty of Veterinary Medicine, Assiut University, Assiut 71526, Egypt.

<sup>3</sup> Department of Pharmaceutics, Faculty of Pharmacy, South Valley University, Qena 83523, Egypt.

**Short Title:** Ameliorative effect of quercetin nanoparticles on hepatotoxicity

**Received:** 25 June 2023; **Accepted:** 18 July 2023

### ABSTRACT

Cyclophosphamide (CYP) is a chemotherapeutic agent used to treat cancers, but its therapeutic uses are limited due to its hepatotoxicity. Consequently, the current work aimed to investigate the potential hepatoprotective impact of quercetin (QRC) nanoparticles against CYP-induced liver damage. Twenty albino rats were divided into four even groups. Group (A) was carried out as the control group. Group (B) injected a single dose of CYP (200 mg/kg) intraperitoneally. Group (C) received orally nano quercetin at a dosage of 50 mg/kg for 10 days, they were also given a single dose of CYP i.p. and Group (D) was given nano-QRC orally at a dose of 50 mg/kg for 10 consecutive days. Samples were collected 24 hours after CYP injection for biochemical, histopathological and ultrastructural examinations. CYP significantly elevated the AST, ALT and MDA levels and substantially reduced the total antioxidant capacity (TAOC) in comparison to the control group. Moreover, the nano-QRC + CYP treated group significantly declined the raised AST and MDA levels, and significantly raised the diminished TAOC as compared to CYP treated group. Histopathological examination revealed a severe degree of congestion and dilatation of the central vein, perivascular fibrosis and hepatocellular vacuolation and necrosis were recorded in CYP treated group. However, only mild hepatic lesions were observed in nano-QRC + CYP treated group. It could be concluded that the administration of nano-QRC ameliorated the hepatic damage induced by CYP via its antioxidant activity.

**Keywords:** Cyclophosphamide, Hepatotoxicity, Histopathology, Oxidative Stress, Quercetin nanoparticles.

### INTRODUCTION

Cyclophosphamide drug (CYP) is one of the chemotherapeutic drugs; Since the

In the 1950s, it has been licensed for use in the treatment of a wide variety of diseases as neoplastic and non-neoplastic disorders for example, solid tumors and lymphomas (Sinanoglu *et al.*, 2012; Mansour *et al.*, 2017), multiple myeloma, leukemias (Abraham and Isaac. 2011), breast cancer (Zhu *et al.*, 2015), ovary adenocarcinoma, prostate cancer (Akamo *et al.*, 2021),

*Corresponding author:* ARMIA N.M. GHALY  
*E-mail address:* [armia\\_naguib@vet.svu.edu.eg](mailto:armia_naguib@vet.svu.edu.eg)  
*Present address:* Department of Pathology and Clinical Pathology, Faculty of Veterinary Medicine, South Valley University, Qena, 83523, Egypt.

neuroblastoma, endometrial cancer (Ayza *et al.*, 2020) and carcinoma of the lung (El Kiki *et al.*, 2020). In addition, it has been used as an immunosuppressive agent in allogeneic bone marrow transplantation (Tuorkey, 2017).

CYP after its administration, it undergoes metabolic activation by cytochrome P450 oxidases in the liver resulting in phosphoramidate mustard (for its anticancer activity) and acrolein (Fouad *et al.*, 2016 and Temel *et al.*, 2020). Acrolein has been identified as a highly toxic substance that causes an increase in reactive oxygen species (ROS), which causes damage to DNA and protein carbonylation, and a disruption in antioxidant defense power by increasing lipid peroxidation and down-regulation the activity of antioxidant enzymes such as superoxide dismutase (SOD), catalase (CAT) and glutathione (GSH) (Patwa *et al.*, 2020 and Lin *et al.*, 2020).

The clinical uses of CYP undergo restricted limitations due to its acrolein metabolites which cause oxidative stress associated with dose-dependent toxicity in different organs such as hepatotoxicity (Aladaileh *et al.*, 2019), urinary bladder toxicity (Ayhanci *et al.*, 2010 and Taha *et al.*, 2015), nephrotoxicity (Temel *et al.*, 2020), ovarian toxicity (Zhang *et al.*, 2018), testicular toxicity (Abarikwu *et al.*, 2012), cardiotoxicity (Komolafe *et al.*, 2020), pulmonary toxicity (Mohamed *et al.*, 2020), bone marrow toxicity (Iqbal *et al.*, 2020) and neurotoxicity (Ibrahim *et al.*, 2021).

Several studies have explored the influence of natural products in reducing or preventing antineoplastic drug toxicity. Polyphenols, which are a key source of antioxidants, are found in several natural goods. Phenolic acid and flavonoids are the two most important kinds of polyphenols (Scalbert *et al.*, 2005). Quercetin (QRC) is a natural antioxidant flavonoid found in abundance in several kinds of foods including fruits, herbs and vegetables like potatoes, apples, soybeans, broccoli, tea, red wine and onions (Ilić *et al.*,

2014 and Bao *et al.*, 2017). Besides its antioxidant capabilities, QRC exhibits anti-inflammatory, analgesic, antidepressant, cholesterol-lowering, metallothionein inducer, anticancer, antihistamine, renal hemodynamic modulator, antiviral, vasodilator and antibacterial properties (Nabavi *et al.*, 2012 and Vicente-Vicente *et al.*, 2019). QRC's antioxidant action is related to its ability to scavenge ROS and suppress lipid peroxidation (Wang *et al.*, 2020). Moreover, several studies have shown that QRC and nano-QRC can protect various organs from damage, including liver damage (Zhang *et al.*, 2019). The purpose of this study was to explore the biochemical and histopathological changes caused by CYP-induced toxicity in rats and explore the protective effect of nano-QRC against CYP-induced toxicity.

## MATERIALS AND METHODS

### 1. Chemical and reagents

Cyclophosphamide (Endoxan) was purchased from Baxter Oncology (Dusseldorf, Germany). Quercetin (cat: Q4951- 10g,  $\geq 95$  purity) and Span 60 were obtained from Sigma-Aldrich Co. (St. Louis, MO, USA). Tween 40 was acquired from El-Nasr Pharmaceutical Chemicals Co. (Cairo, Egypt). The supplier of the ethanol was Merck in Darmstadt, Germany. The additional materials were all of the analytical quality and were purchased from standard commercial sources.

### 2. Formulation of quercetin nanoparticles

QRC nanoparticles were fabricated displaying ethanol injection technique as reported in previous literature (Kakkar and Kaur, 2011 and Fahmy *et al.*, 2018). In brief, calculated amounts of QRC and Span 60 were dissolved in a small amount of ethanol and then infused slowly dropwise into a warmed Tween 40 aqueous solution at 60°C (Span 60:Tween 40 was used at a weight ratio of 3:1). On a magnetic stirrer (made by Thermo Scientific and SA Co., China), the resultant hydroalcoholic solution was continuously

stirred for 30 minutes at 600 rpm till all ethanol is completely evaporated to form QRC-loaded nanoparticles dispersion. The fabricated formulation was stored in a refrigerator (4°C) overnight. Based on a previous study (under publication), different nanoparticle formulations were formulated using different types of spans and edge activators, the optimum formulation containing Tween 40 was selected in this study.

### 3. Laboratory animals and experimental design

Twenty male adult rats (weighting  $180 \pm 20$  gm) at 12-14 weeks of age were obtained from the Assiut University's Animal House, Egypt. The study protocol was authorized by the Animal Ethics Committee of Assiut University's Faculty of Veterinary Medicine in Egypt (approval no 06/2023/0078). Prior to the beginning of the experiment, all animals were allowed to acclimatize in metal cages (5 rats per cage) in a room with good ventilation for 1 week. The rats were kept in standard circumstances, fed a diet of typical commercial pellets and given unlimited access to fresh water.

The Twenty rats were randomly divided into four groups (5 rat/group) as the following:

**Group (A) (control group):** The rats received a single dose of saline intraperitoneally (i.p.) on day 10 of the experiment. **Group (B) (CYP treated group):** The rats were injected single dose of CYP (200 mg/kg) i.p. according to Caglayan *et al.* (2018). **Group (C) (nano-QRC and CYP treated group):** The rats were received orally nano-QRC at a dosage of 50 mg/kg for 10 days. They were also given a single dose of CYP i.p. on day 10 of the experiment (200 mg/kg.bw). **Group (D) (nano-QRC treated group):** The rats were given nano-QRC orally at the dose of 50 mg/kg for 10 consecutive days (Sengul *et al.*, 2017).

### 4. Blood and tissue sampling

At the end of the experiment, all animals from all groups were anaesthetized by inhaling diethyl ether. Blood samples were obtained

through a cardiac puncture and the medial canthus of the eye and then kept in plain tubes for serum analysis. The serum was then collected and kept at  $-20^{\circ}$  C in labeled Eppendorf tubes until it was utilized for determination of liver function test, total antioxidant capacity (TAOC) and malondialdehyde (MDA) levels. Liver tissue specimens have been collected for histopathology examination and transmission electron microscopy.

### 5. Biochemical analysis

AST and ALT enzyme levels were estimated by colorimetric technique which was explained by Reitman and Frankel (1957). Malondialdehyde content (MDA) was assessed by a colorimetric technique which was explained by Ohkawa *et al.* (1979) using a lipid peroxide (malondialdehyde) kit. TAOC was estimated by a colorimetric technique which was explained by Koracevic *et al.* (2001) using TAOC kit. All kits were acquired from Bio Diagnostic Co. Giza, Egypt.

### 6. Histopathological examination

Tissue specimens from the liver were fixed in buffered formalin 10%, dehydrated in an increasing series of ethyl alcohol (70, 80, 90 and 100), and then embedded into paraffin wax according to Bancroft and Gamble (2008). Microscopic examinations involved 5- $\mu$ -thick sections stained with hematoxylin and eosin and Masson's Trichrome stain. The histopathological lesion score is based on the incidence of lesions in 10 examined sections of 5 rats.

### 7. Transmission electron microscopical investigation

Liver specimens were fixed in 5% cold glutaraldehyde for 24-48 hours immediately after animal necropsy, then post-fixed with 1% O4S4 for two hours after being rinsed three to four times for 20 minutes each with cacodylate buffer (pH 7.2), and then washed 4 times with the same buffer. Dehydration with respective ascending alcohol content (30, 50, 70, 90 and 100% for 2 hrs) was done in accordance with Electron Microscope Unit

Assiut University protocol (Bozzola and Russell, 1999) and embedded in epon mixture. LKB ultramicrotome was used to produce semi-thin sections 0.5-1 microns thick cut from embedded blocks, A Leica AG ultramicrotome was used to slice the tissue into ultra-thin sections that were 500–700 Å thick and contrasted as usual with lead citrate and uranyl acetate. The tissue was orientated and then shot using a SC30 Olympus camera. Model XR-41 CCD digital camera with JEM 100 CXII electron microscope at 80 KV was used to inspect and take pictures. Using the program Photo Filter 6.3.2, we digitally colored the TEM pictures in order to identify various cell and structural kinds.

### 8. Statistical analysis

We used SPSS version 26 for statistical analysis of obtained results according to Borenstein *et al.* (1997). The data was expressed as Mean  $\pm$  Standard Error (SE). One-way ANOVA and the post-hoc Tukey HSD test were used for performing multiple comparisons. A difference of  $P \leq 0.05\%$  was considered statistically significant. Graphs were plotted using GraphPad Prism 9.4.1.

## RESULTS

### 1. Biochemical analysis of liver function and oxidative stress markers:

CYP significantly ( $P \leq 0.01$ ) elevated the AST and ALT levels as compared to control rats. While nano-QRC plus CYP treated group was substantially ( $P \leq 0.05$ ) diminished the raised AST levels in comparison to CYP treated group. (Table. 1), (Fig. 1 A, B). Moreover, CYP considerably ( $P \leq 0.05$ ) increased the MDA levels and substantially ( $P \leq 0.05$ ) reduced the TAOC when compared to the control group. While administration of the nano-QRC plus CYP, it significantly ( $P \leq 0.05$ ) declined the raised MDA levels and significantly raised the diminished TAOC versus the CYP-treated group (Table. 2), (Fig. 1 C, D).

### 2. Histopathological examination:

The histopathological evaluations of the liver

tissue sections stained with H&E revealed normal histological structure (Fig. 2 A). The microscopical examination of liver tissue sections stained with H&E stain in CYP treated group revealed vascular and parenchymal changes including severe degree of congestion and dilatation of central vein (Fig. 2 B, C), moderate degree of congestion of portal blood vessel, sinusoidal dilatation, and there was an early perivascular fibroblast proliferation. This perivascular fibrosis was confirmed by using Masson's Trichrome stain and appeared blue in color (Fig. 2 D,E). Moreover, the endothelial cell lining of some blood vessels showed moderate degree of injury. Additionally, the parenchymal changes revealed necrobiotic changes that were expressed by the presence of coagulative necrosis with nuclear and cytoplasmic changes including (pyknosis of nuclei and appeared highly basophilic, fragmentation of nuclear chromatin, and complete disappearance of the nucleus with highly acidophilic cytoplasm) (Fig. 2 C). Vacuolar degeneration of the liver cells in which hepatocyte's cytoplasm contains irregular sizes and shape vacuoles with displacement of nuclei in some vacuolated hepatocytes (Fig. 2 F).

While nano-QRC and CPY treated group revealed mild hepatic lesions as compared to CYP treated group. These lesions included vascular changes such as moderate degree of central vein congestion, mild degree of portal blood vessel congestion, hepatic sinusoidal dilatation, injury to endothelial cell lining, and necrobiotic changes such as vacuolar degeneration and coagulative necrosis of hepatocytes (Fig. 2G,H). The other histopathological findings such as fibrosis that were seen in CYP CYP-treated group weren't observed in the nano-QRC plus CYP-treated group.

Furthermore, there was no significant difference between tissue from the control group and tissue from the nano-QRC only group, in which liver tissue appeared normal (Fig. 2 I). The histopathological grades based on the incidence of lesions in 10 examined

sections of 5 rats (+ Mild lesion present in 1-3 section, ++ moderate lesion present in 4-6 section, and +++ severe lesion present in 7-10 section) were summarized in (Table. 3).

**Transmission electron microscopical findings**  
TEM was performed for liver tissues of CYP treated group, nano-QRC and CYP treated group and control negative group. The TEM examination of hepatic tissue sections from the control negative group showed a normal appearance of the nucleus with prominent nucleoli and normal mitochondria and rough

endoplasmic reticulum (RER) (Fig. 3 A). While, the hepatic tissue sections of the CYP-treated rats by TEM revealed a nucleus with nuclear chromatin lysis, mitochondrial swelling, dilatation and swelling of RER and glycogen depletion (Fig. 3 B,C). However, when nano-QRC were administrated, there was slight alterations were recognized by TEM including hypertrophied Kupffer cells, hepatic sinusoids filled with blood and hepatocytes showing normal mitochondria (Fig. 3D).

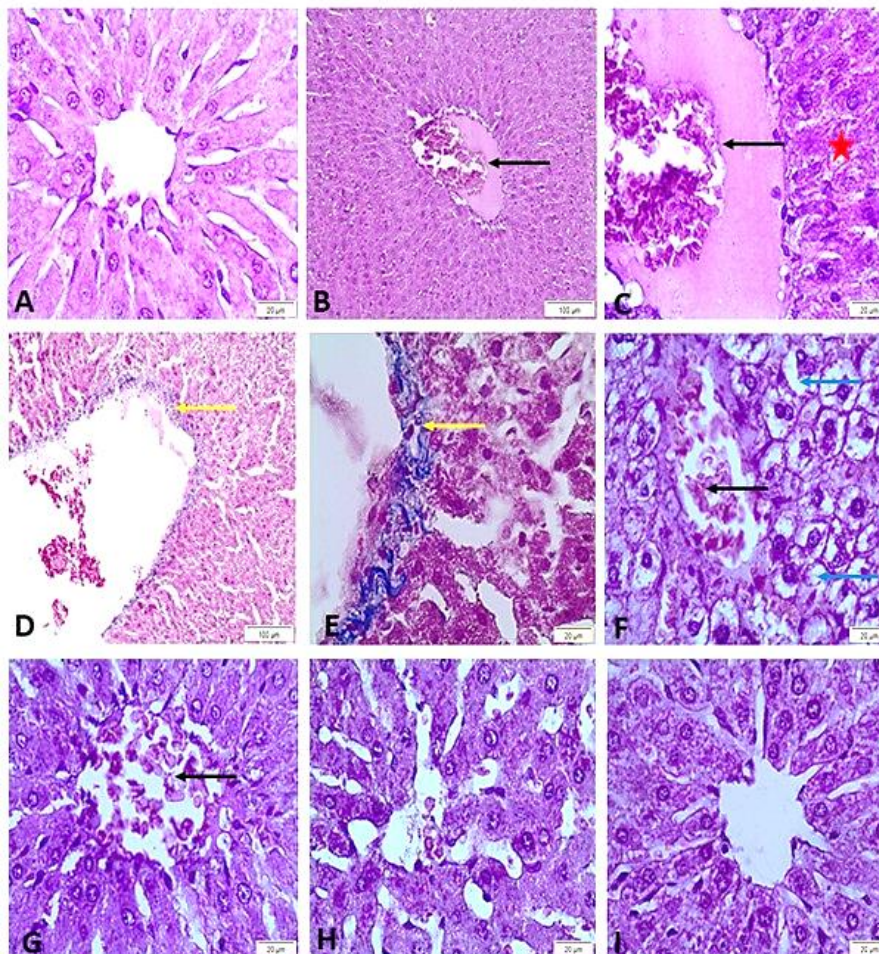


**Fig. 2.** A representative histopathological micrograph of liver tissue sections of rats in all experimental studied groups: (A) Control group showing hepatocytes arranged in cords; with vesicular nucleus and prominent nucleolus and interspersed by hepatic sinusoid. (B-F) CYP treated group showing severe congestion and dilatation of central vein (black arrows), coagulative necrosis of hepatocyte (red stars), perivascular fibrosis appears blue in color (yellow arrows), and vacuolar degeneration of hepatocytes (blue arrows). (G,H) Nano-QRC and CYP treated group showing moderate degree central vein congestion (black arrow), mild degree hepatic sinusoidal dilatation, and coagulative necrosis of hepatocyte. (I) Nano-QRC only treated group showing hepatocyte and blood vessels are normal. (A, B, C, F-I; H&E stain and D & E; Masson's Trichrome stain).

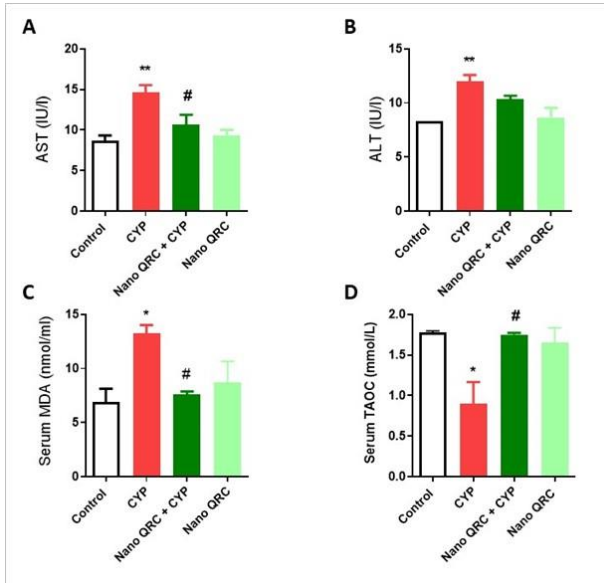


**Fig. 1.** Effect of nano-QRC against a single CYP dose induced hepatotoxicity: (A) AST, (B) ALT, (C) MDA, and (D) TAOC. Data were presented as mean ± S.E, (n = 5). \* P ≤ 0.05, and \*\* P ≤ 0.01 versus Control, and # P ≤ 0.05 versus CYP.

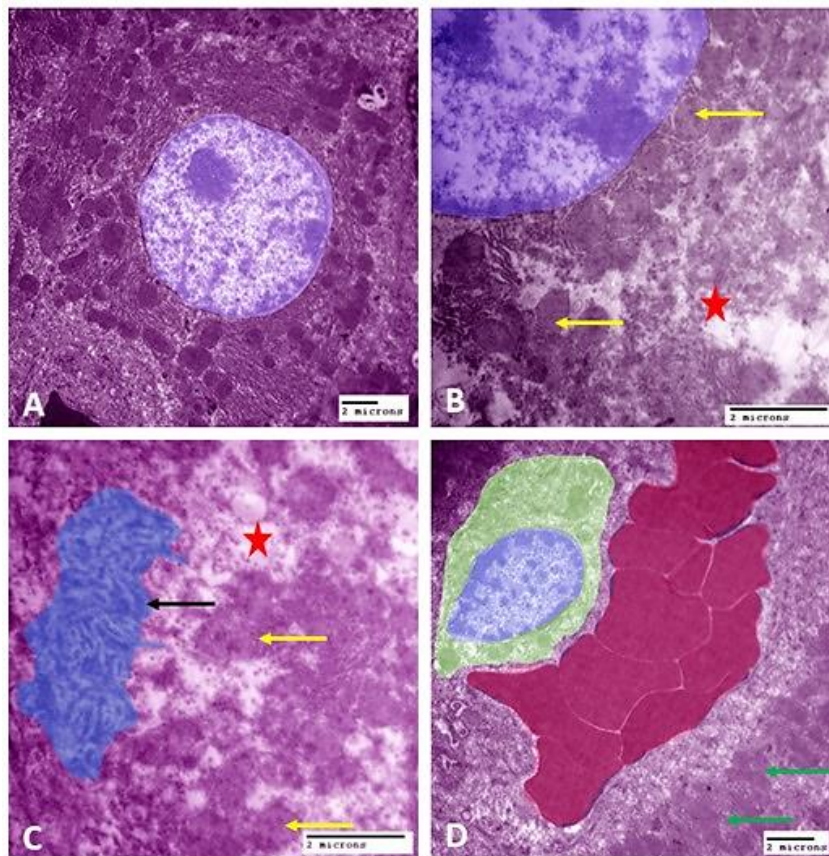


**Fig. 3.** Digitally colored transmission electron micrograph of ultrathin liver tissue sections of rats of the examined groups: (A) Control group showing hepatocytes with typical nuclear appearance with prominent nucleoli and normal mitochondria and RER. (B, C) CYP treated group showing nucleus with nuclear chromatin lysis, mitochondrial swelling (yellow arrows), dilatation and swelling of RER (black arrow), and glycogen depletion (red stars). (D) Nano-QRC and CYP treated group showing hypertrophied Kupffer cells (green color), hepatic sinusoids filled with blood (red color) and normal mitochondria (green arrows).

**Table 1:** Values of liver function tests including AST and ALT in the serum of rats of different groups.

Liver function tests	Group (A) Control group	Group (B) CYP treated group	Group (C) Nano-QRC + CYP treated group	Group (D) Nano-QRC treated group
AST/GOT	8.67 ± 0.67	14.67 ± 0.88 **	10.67 ± 1.20 #	9.33 ± 0.67
ALT/GPT (IU/l)	8.33 ± 0.33	12.00 ± 0.58 **	10.33 ± 0.33	8.67 ± 0.88

\*\* P ≤ 0.01 significantly different versus control group and # P ≤ 0.05 significantly different versus CYP group. Data were presented as mean ± S.E, (n = 5).

**Table 2:** Values of oxidative stress indices including TAOC and MDA level in the serum of rats of different groups.

Oxidative stress biomarkers	Group (A) Control group	Group (B) CYP treated group	Group (C) nano-QRC + CYP treated group	Group (D) nano-QRC treated group
TAOC (mmol/L)	1.78 ± 0.02	0.90 ± 0.27 *	1.75 ± 0.02 #	1.65 ± 0.18
MDA (nmol/ml)	6.91 ± 1.22	13.25 ± 0.77 *	7.61 ± 0.27 #	8.70 ± 1.97

\* P ≤ 0.05 significantly different versus control group and # P ≤ 0.05 significantly different versus CYP group. Data were presented as mean ± S.E, (n = 5).

**Table 3:** The lesion score of histopathological results of the liver in all studied group.

Liver Lesions	Group (A) Control group	Group (B) CYP treated group	Group (C) Nano-QRC + CYP treated group	Group (D) Nano-QRC treated group
• Congestion of C.V <sub>s</sub>	-	+++	++	-
• Congestion of Portal blood vessels	-	++	+	-
• Dilatation of sinusoids	-	+	+	-
• Perivascular fibrosis	-	++	-	-
• Necrobiotic changes	-	++	+	-
• Vacuolar degeneration	-	++	+	-

(- No lesion, + lesion present in 1-3 section, ++ lesion present in 4-6 section, +++ lesion present in 7-10 section.

## DISCUSSION

Cyclophosphamide is a cytotoxic drug widely used for treating different kinds of cancers, but its side effects, such as liver toxicity, limit its therapeutic use (Sinanoglu *et al.*, 2012 and Mostafa *et al.*, 2022). In the present study, a single dose of CYP (200 mg/kg) after 24hrs from the injection, induced a significant rise of the MDA, AST, and ALT levels and substantially reduced the TAOC when compared to control rats, demonstrating oxidative stress. Our obtained data are compliant with Akamo *et al.* (2021) who investigated that rats given single injection of 200 mg/kg of CYP i.p. and sacrificed 24 hours after injection, showed substantially higher serum AST, ALP, ALT and MDA levels. The same result was reported by Cengiz *et al.* (2019) who recorded that the TAOC dramatically decreased in the rats that were previously exposed to CYP at a dose of 200 mg/kg and sacrificed after 3 days. Our observed results also were in conformity with El-Naggar *et al.* (2016) who verified that giving mice 200 mg/kg CYP i.p., altered the hepatic enzymatic system after 5 days from injection as evidenced by a highly substantial rise in AST and ALT levels. Similar finding reported by Nafees *et al.* (2012), that CYP injection 50 mg/kg (i.p.) to mice and after 24hrs, were accompanied by boosted the MDA level, dwindling the antioxidant enzymes' activity and cause breakage to strands of DNA and micronuclei induction.

The liver's antioxidant defense mechanisms deteriorated because of CYP's oxidative metabolism, which generates free radicals like superoxide anion, and hydroxyl radicals (Doustimotlagh *et al.*, 2020). CYP is hydroxylated by hepatic cytochrome P450 enzymes after injection (Voelcker, 2020). Two active metabolites of CYP, notably acrolein and phosphoramidate, are associated with antineoplastic and toxic actions of CYP such as apoptosis, necrosis, and oncosis (Singh *et al.*, 2018). Acrolein weakens the cellular antioxidant defense mechanisms and increases ROS, leading to increased lipid

peroxidation and CYP-associated toxicities (Patwa *et al.*, 2020 and Tohamy *et al.*, 2021).

In our work, the CYP-treated group revealed vascular and parenchymal changes including severe degree of congestion of blood vessels, perivascular fibrosis, and injury of endothelial cell lining of some blood vessels. Additionally, the parenchymal changes include the presence of vacuolar degeneration and hepatocyte coagulative necrosis. Our findings are in harmony with Shokrzadeh *et al.* (2015) and Caglayan *et al.* (2018) who recorded that given single dose of 200 mg/kg.bw of CYP i.p. to rats and sacrificed 24hrs after injection revealed hepatic lesions characterized by severe centrilobular hydropic degeneration and necrosis of hepatocyte as well as sinusoidal dilatations and congested portal area. By contrast, Sherif (2018) reported that after 6 days of injection of CYP at the same dose as our study, the histopathological alteration was periportal fibrosis. Alternatively, Ma *et al.* (2021) stated that the liver displayed hepatocyte necrosis, lymphocyte infiltration, and hepatocyte degeneration, substantial collagen formation in the extracellular matrix after 7 days from injection of CYP.

Our present study confirmed that hepatic damages induced by CYP injection by TEM in hepatic tissue sections of the CYP-treated group revealed the nucleus with nuclear chromatin lysis, mitochondrial swelling, dilatation and swelling of RER and glycogen depletion. Our ultrastructural results agree with Lushnikova *et al.* (2011) and Molodykh *et al.* (2020) who recorded that rat received single CYP dose (125 mg/kg) i.p., after 3 days from CYP injection, revealed several ultrastructural changes, including dilated RER profiles, structural components of the Golgi complex exhibiting hyperplasia and hypertrophy, while some of the ultrastructural changes that take place 14 days later include swelling of mitochondrial with the dilatation of the cristae and focal glycogen lysis. On the other hand, Liu *et al.* (2014) recorded that the ultrastructural changes caused by low doses of CYP (10 mg/kg) for 28 days included

degenerated smaller sized mitochondria with non-obvious cisternae, vesiculated RER and shrunken nuclei with uneven nuclear membranes. Whereas, the injection (20 mg/kg) of CYP for 28 days revealed hepatocytes with an assemblage of heterochromatin, nuclear envelope damage and pyknosis.

Using antioxidants with free radical scavenger activity can help to reduce the harmful effects of chemotherapy drugs (Tohamy *et al.*, 2021). The current work demonstrated that nano-QRC treatment for ten successive days (50 mg/kg) previous to the injection of CYP significantly declined the raised AST and MDA levels and significantly raised up the diminished TAOC in comparison to the CYP-treated group. Moreover, the administration of QRC nanoparticles reflected histologically by the presence of mild hepatic lesions as compared to CYP-treated rats. These lesions included vascular changes such as a moderate degree of central vein congestion, a mild degree of portal blood vessel congestion, hepatic sinusoidal dilatation, injury to endothelial cell lining and necrobiotic changes such as vacuolar degeneration and coagulative necrosis of hepatocytes. While by TEM, there was slight alterations were recognized including hypertrophied Kupffer cells, dilated sinusoids and hepatocytes showing normal mitochondria. Our TEM findings are in harmony with Verma *et al.* (2016) who recorded that nano-QRC was more effective than free QRC for repairing the damaged liver membrane integrity, as evidenced by a significant reduction in blood indicators such as ALT, AST, ALP and LDH and reduced collagen deposition suggested that nano-QRC provided considerably superior advantages than free QRC. The same finding was documented by Ebokaiwe *et al.* (2021) who showed that QRC therapy greatly reduced the high MDA activity, AST and ALT levels caused by CYP, while the antioxidant enzyme capacities that declined, were also restored by QRC. Similarly, Doustimotlagh *et al.* (2020) reported that QRC, particularly when taken before CYP at the dosage of

75mg/kg for 10 successive days, can reduce hepatotoxicity by preventing the peroxidation of lipid, and protein oxidation, as well as restoring the CAT enzyme's activity.

There are several mechanisms through which the nano-QRC can prevent cell death and oxidative stress damage. The mechanisms of hepatoprotective effect of QRC referred to its ability to counteract oxidative stress by chelating metal ions implicated in ROS formation, downregulating ROS producing enzymes, upregulating genes encoding antioxidant enzymes and nuclear factor erythroid 2-related factor 2 (Nrf2) transcription (Rathod *et al.*, 2022). Moreover, the QRC's 3-hydroxyl group was associated with induction of heme oxygenase 1 (HO<sup>-1</sup>). Thus, by activating HO<sup>-1</sup> and strengthening antioxidant capacity, NADPH oxidase-induced inflammation and free radical formation in phagocytic and endothelial cells may be lowered (Luo *et al.*, 2019).

## CONCLUSION

This study demonstrated that i.p. administration of single dose of CYP (200 mg/kg) was induced hepatotoxicity, this was evident by disturbance of oxidative stress indices, liver function indicators, histopathological and abnormal ultrastructural finding. Nano-QRC significantly ameliorated the hepatic damage induced by CYP. These findings suggest the prophylactic therapeutic use of nano-QRC as an independent therapy or in conjunction with cyclophosphamide to mitigate its adverse effects.

## REFERENCES

- Abarikwu, S.O.; Otuechere, C.A.; Ekor, M.; Monwuba, K. and Osobu, D. (2012): Rutin Ameliorates Cyclophosphamide-induced Reproductive Toxicity in Male Rats. *Toxicology International*, 19(2), 207-214.

- Abraham, P. and Isaac, B. (2011): The effects of oral glutamine on cyclophosphamide-induced nephrotoxicity in rats. *Human & experimental toxicology*, 30(7), 616-623.
- Akamo, A.J.; Rotimi, S.O.; Akinloye, D.I.; Ugbaja, R.N.; Adeleye, O.O.; Dosumu, O.A.; Eteng, O.E.; Amah, G.; Obijeku, A. and Cole, O.E. (2021): Naringin prevents cyclophosphamide-induced hepatotoxicity in rats by attenuating oxidative stress, fibrosis, and inflammation. *Food and chemical toxicology*, 153, 112266.
- Aladaileh, S.H.; Abukhalil, M.H.; Saghir, S.A.M.; Hanieh, H.; Alfwuaires, M.A.; Almaiman, A.A.; Bin-Jumah, M. and Mahmoud, A.M. (2019): Galangin Activates Nrf2 Signaling and Attenuates Oxidative Damage, Inflammation, and Apoptosis in a Rat Model of Cyclophosphamide-Induced Hepatotoxicity. *Biomolecules*, 9(8), 346.
- Ayhanci, A.; Yaman, S.; Sahinturk, V.; Uyar, R.; Bayramoglu, G.; Senturk, H.; Altuner, Y.; Appak, S. and Gunes, S. (2010): Protective effect of seleno-L-methionine on cyclophosphamide-induced urinary bladder toxicity in rats. *Biological trace element research*, 134(1), 98-108.
- Ayza, M.A.; Raj Kapoor, B.; Wondafrash, D.Z. and Berhe, A.H. (2020): Protective Effect of Croton macrostachyus (Euphorbiaceae) Stem Bark on Cyclophosphamide-Induced Nephrotoxicity in Rats. *Journal of Experimental Pharmacology*, 12, 275-283.
- Bancroft, J.D. and Gamble, M. (2008): *Theory and practice of histological techniques*: Elsevier health sciences.
- Bao, D.; Wang, J.; Pang, X. and Liu, H. (2017): Protective Effect of Quercetin against Oxidative Stress-Induced Cytotoxicity in Rat Pheochromocytoma (PC-12) Cells. *Molecules*, 22(7), 1122.
- Borenstein, M.; Rothstein, H. and Cohen, J. (1997): Analysis of variance. *SPSS Inc., Chicago*.
- Bozzola, J.J. and Russell, L.D. (1999). *Electron microscopy: principles and techniques for biologists*: Jones & Bartlett Learning.
- Caglayan, C.; Temel, Y.; Kandemir, F.M.; Yildirim, S. and Kucukler, S. (2018): Naringin protects against cyclophosphamide-induced hepatotoxicity and nephrotoxicity through modulation of oxidative stress, inflammation, apoptosis, autophagy, and DNA damage. *Environmental Science and Pollution Research*, 25, 20968-20984.
- Cengiz, M.; Cetik Yildiz, S.; Demir, C.; Sahin, I. K.; Teksoy, O. and Ayhanci, A. (2019): Hepato-preventive and anti-apoptotic role of boric acid against liver injury induced by cyclophosphamide. *Journal of Trace Elements in Medicine and Biology*, 53, 1-7.
- Doustimotlagh, A.H.; Kokhdan, E.P.; Vakilpour, H.; Khalvati, B.; Barmak, M.J.; Sadeghi, H. and Asfaram, A. (2020): Protective effect of Nasturtium officinale R. Br and quercetin against cyclophosphamide-induced hepatotoxicity in rats. *Molecular Biology Reports*, 47(7), 5001-5012.
- Ebokaiwe, A.P.; Obasi, D.O.; Njoku, R.C.C.; Osawe, S.; Olusanya, O. and Kalu, W.O. (2021): Cyclophosphamide instigated hepatic-renal oxidative/inflammatory stress aggravates immunosuppressive indoleamine 2,3-dioxygenase in male rats: Abatement by quercetin. *Toxicology*, 464.
- El-Naggar, S.A.; Abdel-Farid, I.B.; Germoush, M.O.; Elgebaly, H.A. and Alm-Eldeen, A.A. (2016): Efficacy of Rosmarinus officinalis leaves extract against cyclophosphamide-induced hepatotoxicity. *Pharmaceutical biology*, 54(10), 2007-2016.
- El Kiki, S.M.; Omran, M.M.; Mansour, H.H. and Hasan, H.F. (2020): Metformin and/or low dose radiation reduces

- cardiotoxicity and apoptosis induced by cyclophosphamide through SIRT-1/SOD and BAX/Bcl-2 pathways in rats. *Molecular Biology Reports*, 47(7), 5115-5126.
- Fahmy, A.M.; El-Setouhy, D.A.; Ibrahim, A.B.; Habib, B.A.; Tayel, S.A. and Bayoumi, N.A. (2018): Penetration enhancer-containing spanlastics (PECSs) for transdermal delivery of haloperidol: in vitro characterization, ex vivo permeation and in vivo biodistribution studies. *Drug delivery* 25(1), 12-22.
- Fouad, A.A.; Qutub, H.O. and Al-Melhim, W.N. (2016): Punicalagin alleviates hepatotoxicity in rats challenged with cyclophosphamide. *Environmental Toxicology and Pharmacology*, 45, 158-162.
- Ibrahim, H.M.; Zommara, M.A.E. and Elnaggar, M.E. (2021): Ameliorating effect of selenium nanoparticles on cyclophosphamide-induced hippocampal neurotoxicity in male rats: light, electron microscopic and immunohistochemical study. *Folia morphologica*, 30(4), 806-819.
- Ilić, S.; Stojiljković, N.; Veljković, M.; Veljković, S. and Stojanović, G. (2014): Protective effect of quercetin on cisplatin-induced nephrotoxicity in rats. *Facta Universitatis, Series: Medicine and Biology*, 16(2), 71-75.
- Iqbal, A.; Syed, M.A.; Haque, M.M.; Najmi, A.K.; Ali, J. and Haque, S.E. (2020): Effect of nerolidol on cyclophosphamide-induced bone marrow and hematologic toxicity in Swiss albino mice. *Experimental Hematology*, 82, 24-32.
- Kakkar, S. and Kaur, I.P. (2011): Spanlastics--a novel nanovesicular carrier system for ocular delivery. *International journal of pharmaceutics* 413(1-2), 202-210.
- Komolafe, O.A.; Arayombo, B.E.; Abiodun, A.A.; Saka, O.S.; Abijo, A.Z.; Ojo, S.K. and Fakunle, O.O. (2020): Immunohistochemical and histological evaluations of cyclophosphamide-induced acute cardiotoxicity in Wistar rats: The role of turmeric extract (Curcuma). *Morphologie*, 104(345), 133-142.
- Koracevic, D.; Koracevic, G.; Djordjevic, V.; Andrejevic, S. and Cosic, V. (2001): Method for the measurement of antioxidant activity in human fluids. *Journal of Clinical Pathology*, 54(5), 356-361.
- Lin, X.; Yang, F.; Huang, J.; Jiang, S.; Tang, Y. and Li, J. (2020): Ameliorate effect of pyrroloquinoline quinone against cyclophosphamide-induced nephrotoxicity by activating the Nrf2 pathway and inhibiting the NLRP3 pathway. *Life Sciences*, 256, 117901.
- Liu, W.; Gao, F. F.; Li, Q.; Lv, J. W.; Wang, Y.; Hu, P. C.; Xiang, Q. M. and Wei, L. (2014): Protective effect of astragalus polysaccharides on liver injury induced by several different chemotherapeutics in mice. *Asian Pacific Journal of Cancer Prevention*, 15(23), 10413-14020.
- Luo, M.; Tian, R.; Yang, Z.; Peng, Y. Y. and Lu, N. (2019): Quercetin suppressed NADPH oxidase-derived oxidative stress via heme oxygenase-1 induction in macrophages. *Archives of biochemistry and biophysics*, 671, 69-76.
- Lushnikova, E.L.; Molodykh, O.P.; Nepomnyashchikh, L.M.; Bakulina, A.A. and Sorokina, Y.A. (2011): Ultrastructural picture of cyclophosphamide-induced damage to the liver. *Bulletin of Experimental Biology and Medicine*, 151(6), 751-756.
- Ma, X.; Ruan, Q.; Ji, X.; Yang, J. and Peng, H. (2021): Ligustrazine alleviates cyclophosphamide-induced hepatotoxicity via the inhibition of Txnip/Trx/NF-kappaB pathway. *Life Sciences*, 274, 119331.
- Mansour, D.F.; Saleh, D.O. and Mostafa, R.E. (2017): Genistein Ameliorates Cyclophosphamide - Induced Hepatotoxicity by Modulation of Oxidative Stress and Inflammatory

- Mediators. *Open access Macedonian Journal of medical sciences*, 5(7), 836-843.
- Mohamed, M.T.; Zaitone, S.A.; Ahmed, A.; Mehanna, E.T. and El-Sayed, N.M. (2020): Raspberry Ketones Attenuate Cyclophosphamide-Induced Pulmonary Toxicity in Mice through Inhibition of Oxidative Stress and NF-KappaB Pathway. *Antioxidants*, 9(11), 1168.
- Molodykh, O.P.; Sorokina, I.V.; Vinogradova, E.V.; Kapustina, V.I. and Khodakov, A.A. (2020): Ultrastructure of the Liver in Response to Cyclophosphamide and Triterpenoids. *Bulletin of Experimental Biology and Medicine*, 168(3), 400-405.
- Mostafa, R.E.; Morsi, A.H. and Asaad, G.F. (2022): Piracetam attenuates cyclophosphamide-induced hepatotoxicity in rats: Amelioration of necroptosis, pyroptosis and caspase-dependent apoptosis. *Life Sciences*, 303, 120671.
- Nabavi, S.F.; Nabavi, S.M.; Mirzaei, M. and Moghaddam, A.H. (2012): Protective effect of quercetin against sodium fluoride-induced oxidative stress in rat's heart. *Food & function*, 3(4), 437-441.
- Nafees, S.; Ahmad, S. T.; Arjumand, W.; Rashid, S.; Ali, N. and Sultana, S. (2012): Modulatory effects of genticic acid against genotoxicity and hepatotoxicity induced by cyclophosphamide in Swiss albino mice. *Journal of Pharmacy and Pharmacology*, 64(2), 259-267.
- Ohkawa, H.; Ohishi, N. and Yagi, K. (1979): Assay for lipid peroxides in animal tissues by thiobarbituric acid reaction. *Analytical Biochemistry*, 95(2), 351-358.
- Patwa, J.; Khan, S. and Jena, G. (2020): Nicotinamide attenuates cyclophosphamide-induced hepatotoxicity in SD rats by reducing oxidative stress and apoptosis. *Journal of Biochemical and molecular toxicology*, 34(10), e22558.
- Rathod, S.; Arya, S.; Kanike, S.; Shah, S. A.; Bahadur, P. and Tiwari, S. (2022): Advances on nanoformulation approaches for delivering plant-derived antioxidants: A case of quercetin. *International Journal of Pharmaceutics*, 625, 122093.
- Reitman, S. and Frankel, S. (1957): A colorimetric method for the determination of serum glutamic oxalacetic and glutamic pyruvic transaminases. *American journal of clinical pathology*, 28(1), 56-63.
- Scalbert, A.; Manach, C.; Morand, C.; Remesy, C. and Jimenez, L. (2005): Dietary polyphenols and the prevention of diseases. *Critical Reviews in Food Science and Nutrition*, 45(4), 287-306.
- Sengul, E.; Gelen, V.; Gedikli, S.; Ozkanlar, S.; Gur, C.; Celebi, F. and Cinar, A. (2017): The protective effect of quercetin on cyclophosphamide-Induced lung toxicity in rats. *Biomedicine & Pharmacotherapy*, 92, 303-307.
- Sherif, I.O. (2018): The effect of natural antioxidants in cyclophosphamide-induced hepatotoxicity: Role of Nrf2/HO-1 pathway. *International immunopharmacology*, 61, 29-36.
- Shokrzadeh, M.; Chabra, A.; Ahmadi, A.; Naghshvar, F.; Habibi, E.; Salehi, F. and Assadpour, S. (2015): Hepatoprotective effects of zataria multiflora ethanolic extract on liver toxicity induced by cyclophosphamide in mice. *Drug research*, 65(4), 169-175.
- Sinanoglu, O.; Yener, A.N.; Ekici, S.; Midi, A. and Aksungar, F.B. (2012): The protective effects of spirulina in cyclophosphamide-induced nephrotoxicity and urotoxicity in rats. *Urology*, 80(6), 1392 e1391.
- Singh, C.; Prakash, C.; Tiwari, K. N.; Mishra, S.K. and Kumar, V. (2018): *Premna integrifolia* ameliorates cyclophosphamide-induced hepatotoxicity by modulation of oxidative stress and apoptosis.

- Biomedicine & Pharmacotherapy*, 107, 634-643.
- Taha, N.R.; Amin, H.A. and Sultan, A.A. (2015): The protective effect of *Moringa oleifera* leaves against cyclophosphamide-induced urinary bladder toxicity in rats. *Tissue and Cell*, 47(1), 94-104.
- Temel, Y.; Kucukler, S.; Yildirim, S.; Caglayan, C. and Kandemir, F.M. (2020): Protective effect of chrysin on cyclophosphamide-induced hepatotoxicity and nephrotoxicity via the inhibition of oxidative stress, inflammation, and apoptosis. *Naunyn-Schmiedeberg's archives of pharmacology*, 393(3), 325-337.
- Tohamy, A.F.; Hussein, S.; Moussa, I.M.; Rizk, H.; Daghash, S.; Alsubki, R.A.; Mubarak, A.S.; Alshammari, H.O.; Al-Maary, K.S. and Hemeg, H.A. (2021): Lucrative antioxidant effect of metformin against cyclophosphamide-induced nephrotoxicity. *Saudi Journal of Biological Sciences*, 28(5), 2755-2761.
- Tuorkey, M.J. (2017): Therapeutic Potential of *Nigella sativa* Oil Against Cyclophosphamide-Induced DNA Damage and Hepatotoxicity. *Nutrition and cancer*, 69(3), 498-504.
- Verma, S.K.; Rastogil, S.; Arora, I.; Javed, K.; Akhtar, M. and Samim, M. (2016): Nanoparticle-Based Delivery of Quercetin for the Treatment of Carbon Tetrachloride Mediated Liver Cirrhosis in Rats. *Journal of Biomedical Nanotechnology*, 12(2), 274-285.
- Vicente-Vicente, L.; González-Calle, D.; Casanova, A. G.; Hernández-Sánchez, M.T.; Prieto, M.; Rama-Merchán, J.C.; Martín-Moreiras, J.; Martín-Herrero, F.; Sánchez, P.L. and López-Hernández, F.J. (2019): Quercetin, a promising clinical candidate for the prevention of contrast-induced nephropathy. *International journal of molecular sciences*, 20(19), 4961.
- Voelcker, G. (2020): The mechanism of action of cyclophosphamide and its consequences for the development of a new generation of oxazaphosphorine cytostatics. *Scientia Pharmaceutica*, 88(4), 42.
- Wang, J.; Zhu, H.; Wang, K.; Yang, Z. and Liu, Z. (2020): Protective effect of quercetin on rat testes against cadmium toxicity by alleviating oxidative stress and autophagy. *Environmental Science and Pollution Research*, 27, 25278-25286.
- Zhang, B.F.; Hu, Y.; Liu, X.; Cheng, Z.; Lei, Y.; Liu, Y.; Zhao, X.; Mu, M.; Yu, L. and Cheng, M.L. (2018): The role of AKT and FOXO3 in preventing ovarian toxicity induced by cyclophosphamide. *PLoS One*, 13(8), e0201136.
- Zhang, Q.; Xu, D.; Guo, Q.; Shan, W.; Yang, J.; Lin, T.; Ye, S.; Zhou, X.; Ge, Y.; Bi, S. and Ren, L. (2019): Theranostic Quercetin Nanoparticle for Treatment of Hepatic Fibrosis. *Bioconjugate Chemistry*, 30(11), 2939-2946.
- Zhu, H.; Long, M.H.; Wu, J.; Wang, M.M.; Li, X.Y.; Shen, H.; Xu, J.D.; Zhou, L.; Fang, Z.J.; Luo, Y. and Li, S.L. (2015): Ginseng alleviates cyclophosphamide-induced hepatotoxicity via reversing disordered homeostasis of glutathione and bile acid. *Scientific Reports*, 5(1), 1-14.

## التأثير التحسيني لجزيئات الكيرسيتين النانوية على السمية الكبدية المستحثة بواسطة السيكلوفوسفاميد في الجرذان

ارميا نجيب معتمد ، مختار طه ، عبير سعد حسن ، خالد محمد أحمد حسنين

Email: armia\_naguib@vet.svu.edu.eg Assiut University web-site: [www.aun.edu.eg](http://www.aun.edu.eg)

الهدف من هذه الدراسة هو استكشاف التأثير الوقائي المحتمل لجزيئات الكيرسيتين النانوية ضد التلف الكبدي الناجم عن عقار السيكلوفوسفاميد. تم تقسيم عشرين جرذاً إلى أربع مجموعات (٥ جرذ / مجموعة). المجموعة (أ) بمثابة مجموعة ضابطة. المجموعة (ب) أعطيت جرعة واحدة من السيكلوفوسفاميد (٢٠٠ مجم / كجم) داخل الصفاق، بينما تلقت المجموعة (ج) نانو كيرسيتين عن طريق الفم بجرعة ٥٠ مجم / كجم لمدة ١٠ أيام، بالإضافة إلى جرعة واحدة من جرعة السيكلوفوسفاميد في اليوم العاشر من التجربة. والمجموعة (د) تم إعطاؤها نانو كيرسيتين عن طريق الفم بجرعة ٥٠ مجم / كجم لمدة ١٠ أيام متتالية. بعد أربعة وعشرين ساعة من حقن السيكلوفوسفاميد، تم جمع العينات لأجراء التحاليل البيوكيميائية، ولل فحص التشريحي المرضي للأنسجة، والتحليل الدقيق بالميكروسكوب الإلكتروني النافذ. أظهرت النتائج البيوكيميائية أن السيكلوفوسفاميد رفع بشكل ملحوظ من مستويات الأسبارتات أمينوترانسفيراز، ألانين ترانس أميناز، والمالونديالدهيد وقل بشكل كبير من قدرة مضادات الأكسدة الكلية مقارنة بالمجموعة الضابطة. علاوة على ذلك، أدت المعالجة بجزيئات الكيرسيتين النانوية والسيكلوفوسفاميد إلى تضائل كبير في مستويات الأسبارتات أمينوترانسفيراز المرتفعة والمالونديالدهيد ورفعت بشكل ملحوظ القدرة الكلية المضادة للأكسدة المتناقصة مقارنة بالمجموعة المعالجة بالسيكلوفوسفاميد. أظهر الفحص النسيجي المرضي درجة شديدة من الاحتقان وتمدد الوريد المركزي ونخر تخثر الخلايا الكبدية والتليف المحيط بالأوعية الدموية بعد حقن السيكلوفوسفاميد، ومع ذلك، لوحظ فقط الأفات الكبدية الخفيفة في المجموعة المعالجة بجزيئات الكيرسيتين النانوية. نستخلص من هذه الدراسة أن إعطاء جزيئات الكيرسيتين النانوية يحسن التلف الكبدي الناجم عن عقار السيكلوفوسفاميد وذلك لتأثيره المضاد للأكسدة.